

# New insight into the physics of the “sawtooth oscillation” via 2-D visualization

Hyeon K. Park

Princeton Plasma Physics Laboratory

Princeton University

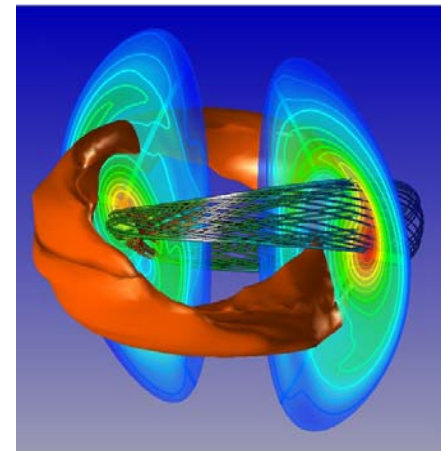
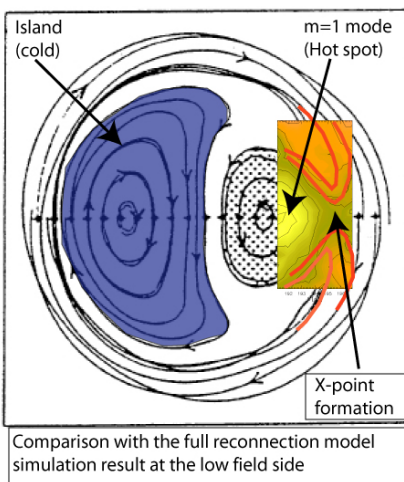
at

16<sup>th</sup> International Toki Conference

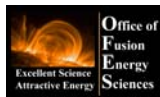
(Advanced Imaging and Plasma Physics)

Ceratopia Toki, Gifu, Japan

December 5-8, 2006



Supported by



Office of Science



Colorado  
University of Colorado at Boulder

## 2-D visualization in plasma physics

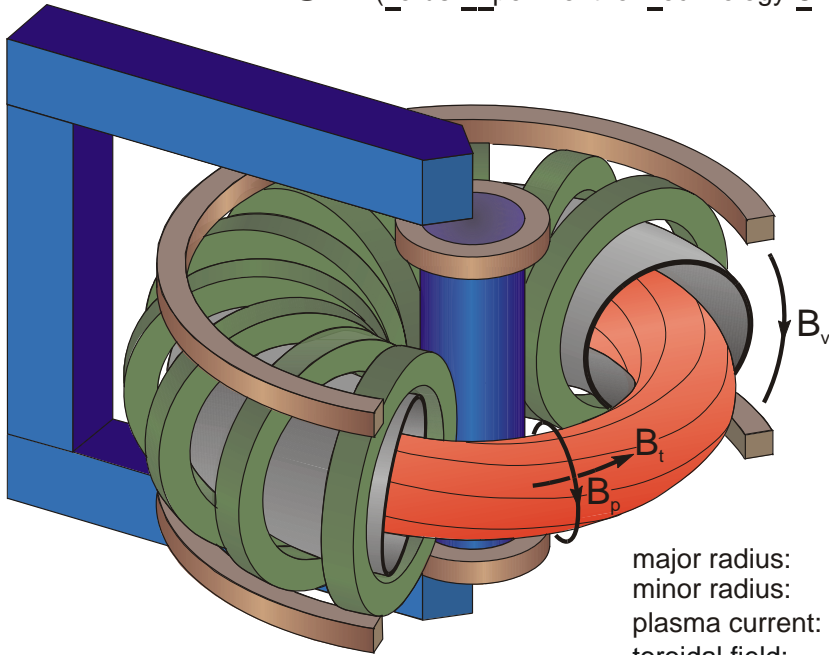
- ❑ Experimental verification of the hypothesis and assumptions is essential for the advancement of science
- ❑ Comprehensive visualization is the best tool for the verification of complex phenomena in science

# Talk

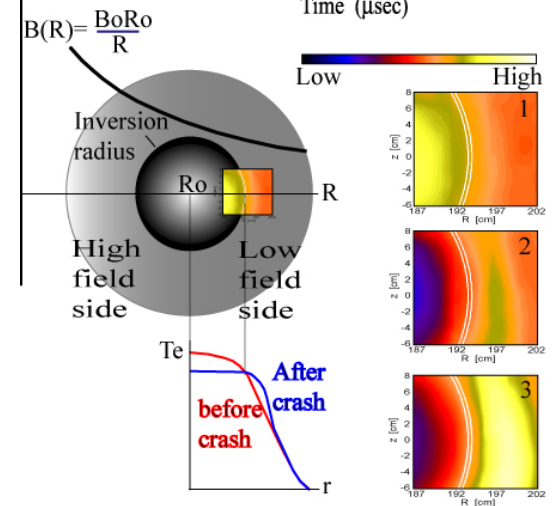
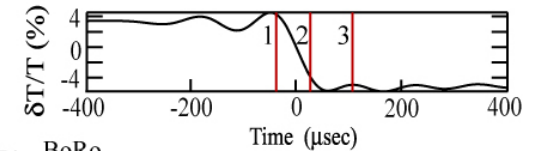
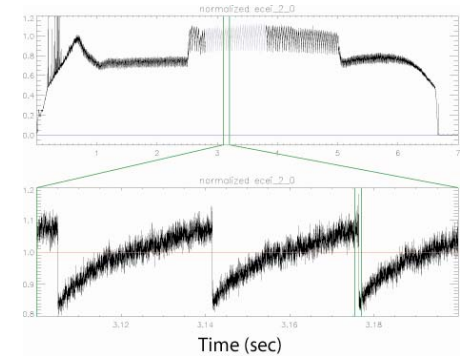
- ❑ Magnetic reconnection process of the  $m/n=1/1$  mode (“sawtooth oscillation”) in hot plasmas
  - ❑ Brief background of the magnetic reconnection process
  - ❑ Prominent theoretical models for the “sawtooth oscillation” for the last ~30 years
  
- ❑ Visualization of  $T_e$  fluctuations in high temperature plasmas for the fundamental physics of the complex plasma dynamics
  - ❑ High resolution (temporal and spatial) 2-D images
  
- ❑ New insight into the physics of the “sawtooth oscillation” via 2-D visualization
  - ❑ New findings of the physics of “sawtooth oscillation” (*PRLs, 96, 195003 & 195004, '06 and PoP, 13,55907, '06*)
  - ❑ 3-D random localized reconnection process

# Classical $m/n=1/1$ instability (sawtooth oscillation)

**TEXTOR** (Torus-Experiment for Technology Oriented Research)



major radius: 1.75 m  
 minor radius: 0.50 m  
 plasma current:  $\leq 0.5$  (0.8) MA  
 toroidal field:  $\leq 2.8$  T  
 pulse length:  $\leq 10$  sec

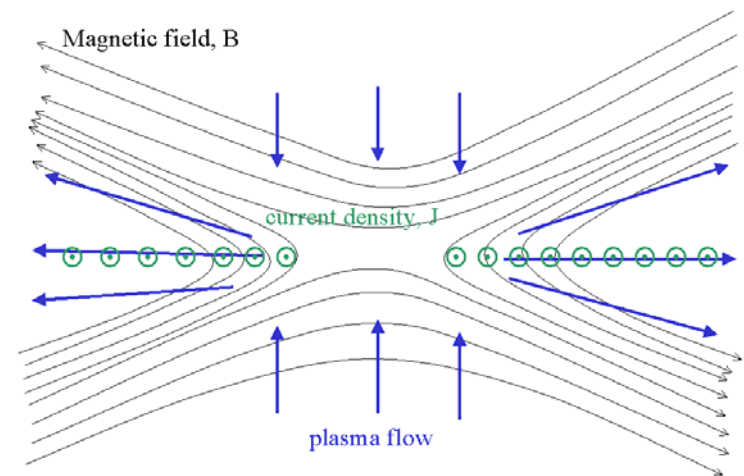
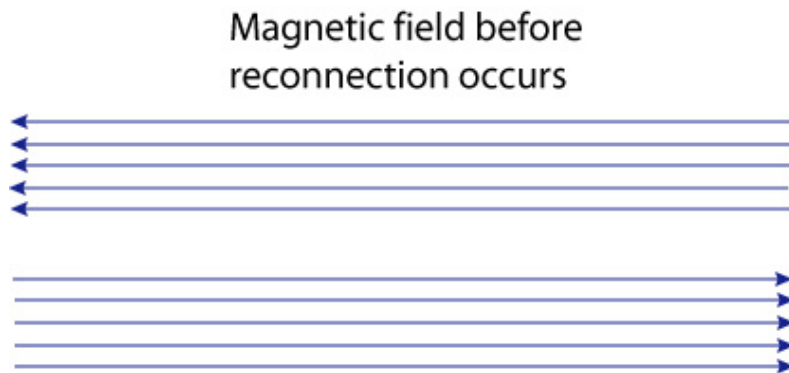


- Sawtooth oscillation is a magnetic self-organization via reconnection

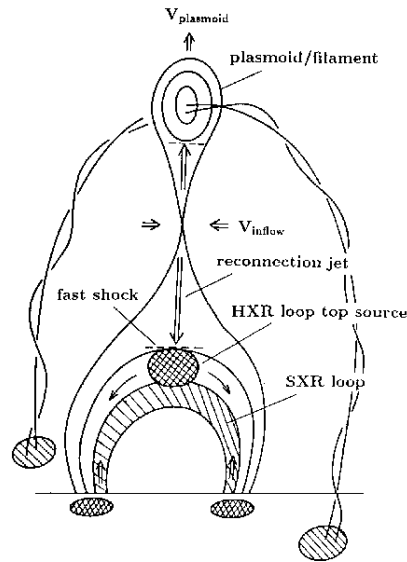
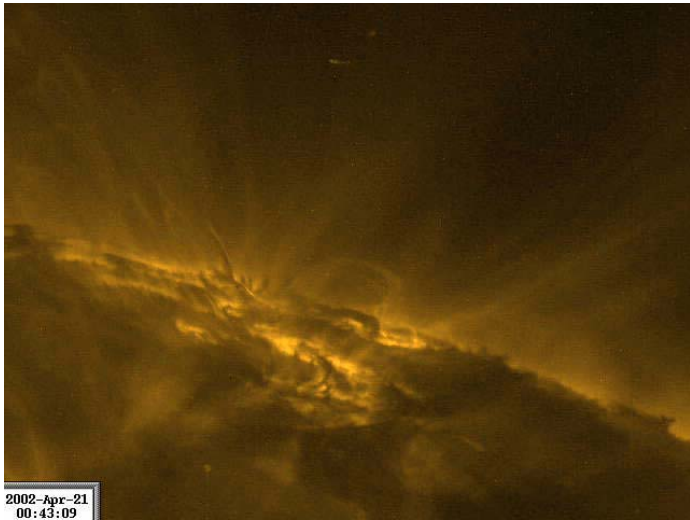


# What is the magnetic reconnection process?

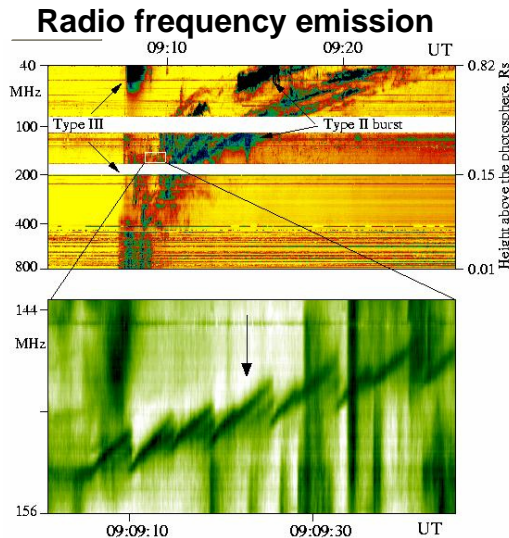
- ❑ *Topological changes of magnetic domain occur when two magnetic surfaces with an opposite direction are merged*
- ❑ *Once the reconnection process takes place, the speed is an order magnitude faster than theoretical model derived from the first principle*
  - ❑ *Magnetic energy can be removed and plasma pressure can be redistributed through the modified local magnetic lines*
  - ❑ *Electron temperature is known to be well tied to the magnetic field line*



# Reconnection process phenomena



Discovery of Loop top HXR source led to **Unified model** (Shibata et al 1995)



Klassen et al.  
A.A. 370 (3)  
\_41-L44,2001

- Striking similarity of the sawtooth crash between tokamak and solar flare plasmas

# Sawtooth oscillation and full reconnection model

- Sawtooth oscillation: a periodic growth (*long*) and decay (*sudden*) of the core pressure of the toroidal plasma (S. von Goeler, '74):
- Full reconnection model (B. Kadomtsev, '76)
  - $m/n=1/1$  mode becomes unstable for  $q(0) < 1$ , where  $q$  represent a degree of the helical twist of the magnetic field line
  - Pressure driven instability near the steepened pressure gradient region due to the kink motion of the  $m/n=1/1$  mode leads to the reconnection

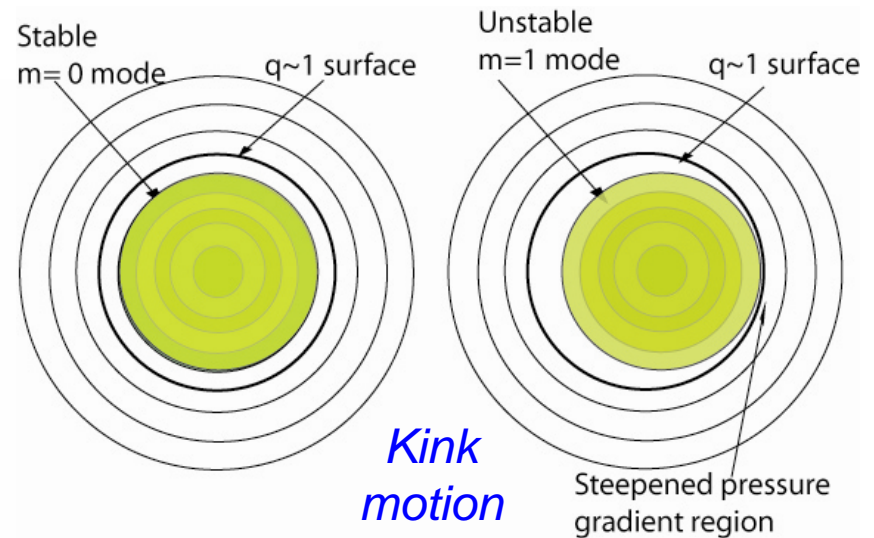
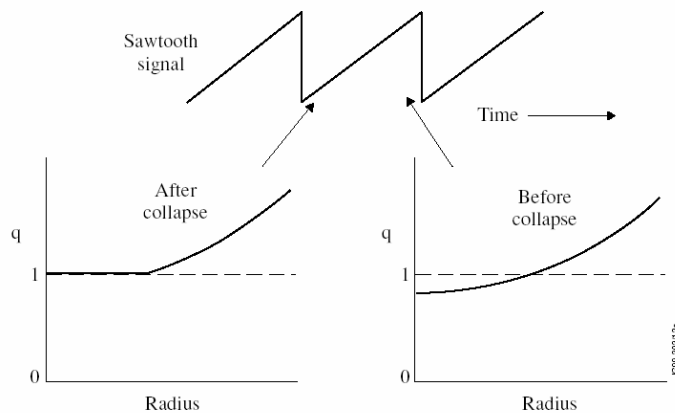


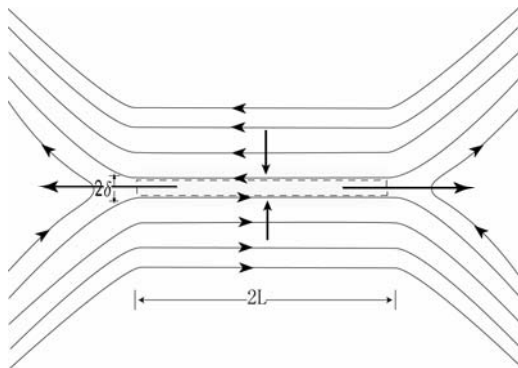
Figure 10.12. Kadomtsev's model predicts a flattening of the  $q$ -profile at the sawtooth collapse and the development of an unstable profile with  $q < 1$  during the ramp phase.

# Sawtooth oscillation and full reconnection model

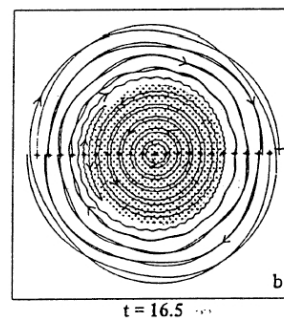
## □ Helically symmetric reconnection zone (*hypothesis*)

- Y-point reconnection process (2-D Sweet-Parker model)
- Long reconnection time (monotonic full growth of the island)
- New model is inevitable because

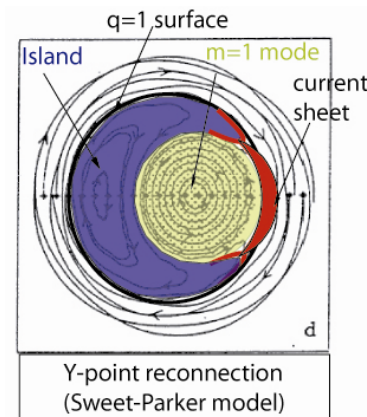
- Measured crash time was much shorter than the predicted value
- Crash occurs without full growth of the island
- ICRF driven giant sawtooth and precursor less sawtooth



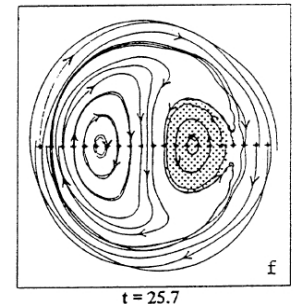
2-D Sweet-Parker model  
(Y-point reconnection)



$$\tau_k \approx \frac{1}{2} \sqrt{\tau_A^* \cdot \tau_\eta}$$

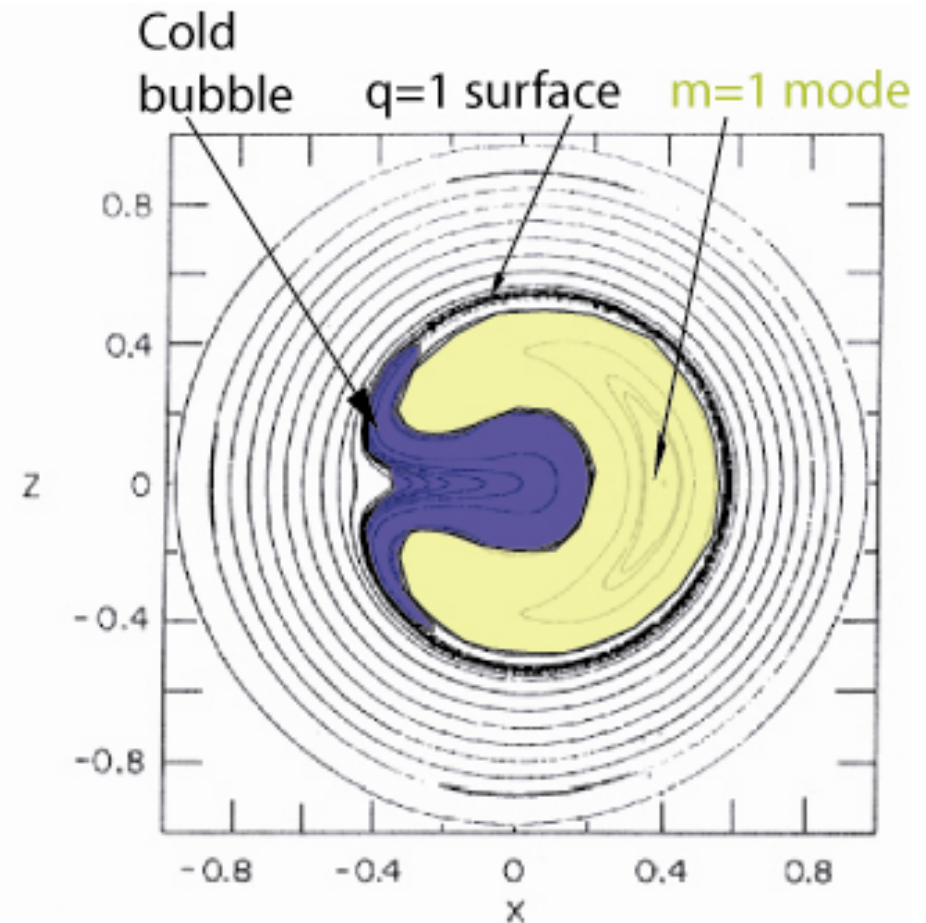


Sykes et al. *PRL*, 36, 140, 1976  
based on MHD fluid in cylindrical geometry



# Sawtooth oscillation and quasi-interchange mode

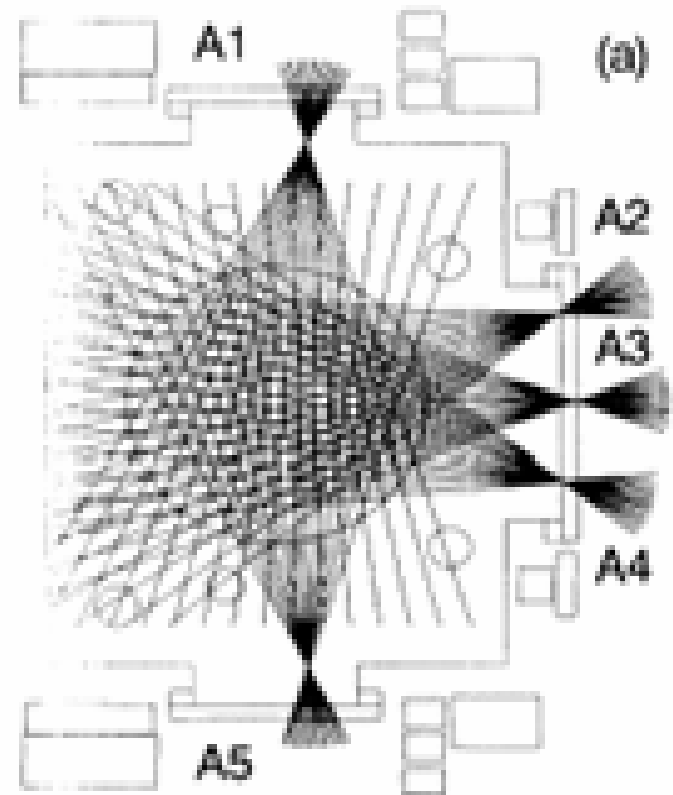
- ❑ Quasi-interchange mode model (J. Wesson, '86) triggered by magnetic instability
- ❑ Constant  $q(0) \sim 1$  and no reconnection process
- ❑ *Distinctive cold bubble shape is contrast to the island shape of the full reconnection model*
- ❑ This model was initially confirmed by x-ray tomography of the JET plasma (Granetz, '88)





# Sawtooth oscillation and quasi-interchange mode

- ❑ Reconstruction of 2-D and 3-D images from limited X-ray arrays
  - ❑ *Inversion process is complex and unique solution may not be feasible with small number of chords*
  - ❑ *Parametric dependence of the X-ray signal adds more complexity ( $T_e$ ,  $n_e$  and  $Z_{eff}$ )*
- ❑ *Full reconnection or interchange model dependent upon number of polynomial in inversion process (C. Janicki '89)*



# Experimental verification of q-profile

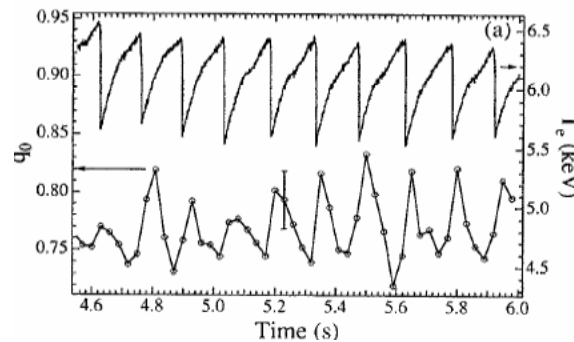
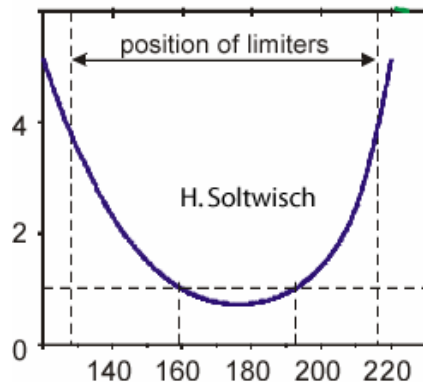
## □ Current profiles

- Central q value remains at  $\sim 0.7$  (TEXTOR; H. Soltwisch, '88 & TFTR; F. Levinton, '94)

## □ Little changes in the measured magnetic energy contradicts to the previous theoretical models

## □ Leads to new idea – Ballooning mode model

Measured q profile on TEXTOR



*A part of stored magnetic energy is released during the crash period of  $100 \mu\text{sec} \ll \tau_{sp}$  (TFTR)*

# Sawtooth oscillation and ballooning mode model

- Ballooning modes (“pressure finger”) predominantly at the low field side can lead to a localized reconnection
- Global stochastic magnetic field (**hypothesis**) is introduced for slow magnetic energy release and fast heat transport
- Consistent with the 3-D local reconnection model (Yamada & Nagayama, et al., '94)

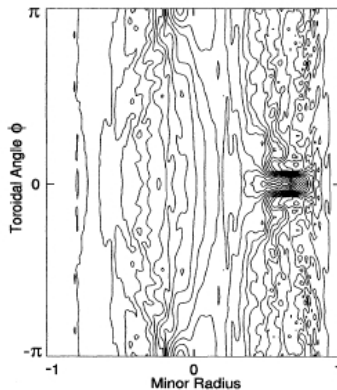


FIG. 5. The pressure contours on the midplane of the torus.

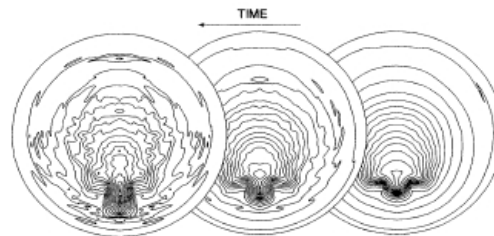


FIG. 4. The nonlinear time development of the pressure.

W. Park, et al. ('96)

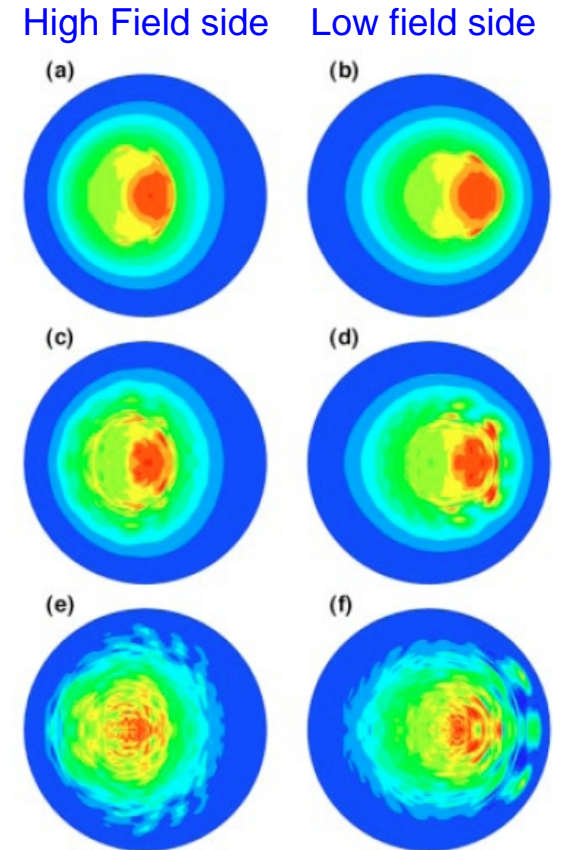
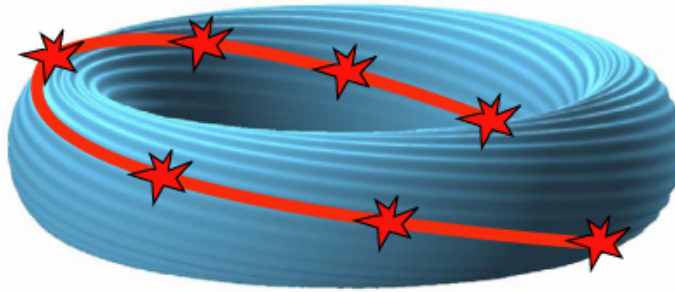


FIG. 2. Pressure contours for the  $\beta=4\%$  simulation. The axisymmetry center line is located at the middle of the page. (a), (b) at  $t=1.205 \times 10^{-2}$ , (c), (d) at  $t=1.230 \times 10^{-2}$ , and (e), (f) at  $t=1.265 \times 10^{-2}$ .

Y. Nishimura, et al. ('99)

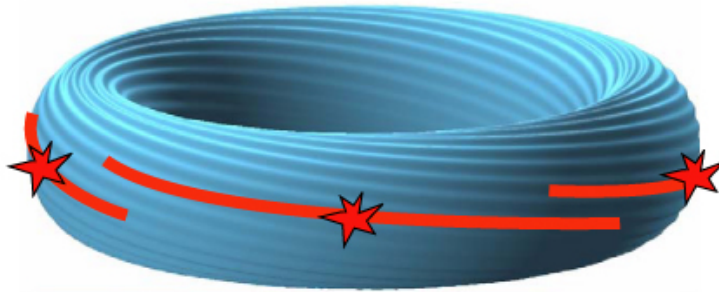


# Studies suggest a 3-D localized reconnection



Full reconnection (Helically symmetric crash)

***Kadomtsev model predicted a full reconnection (pressure and magnetic energy are changing together)***



3-D Local reconnection (localized crash at low field side)

***Localized  $T_e$  breakup; Y. Nagayama '94),***

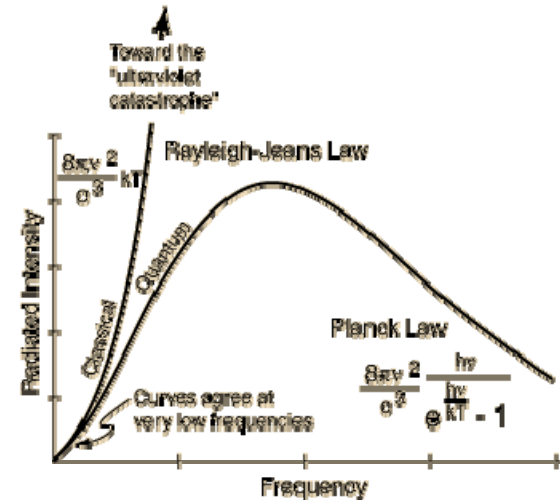
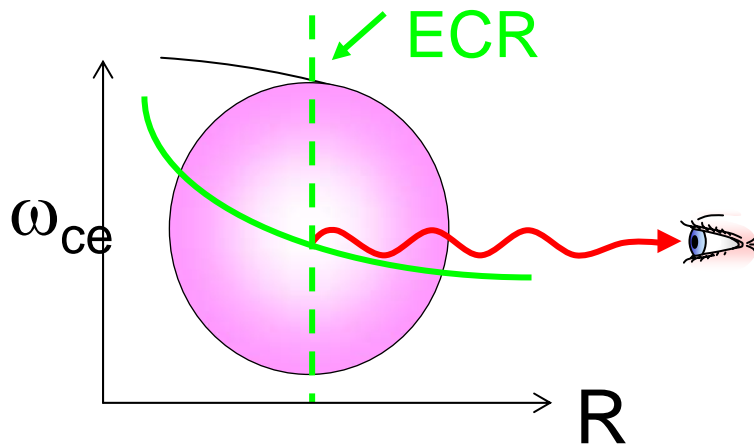
***Little magnetic energy change; (Levinton, '94)***

***⇒ Ballooning based models***

***W. Park et al. & Y. Nishimura et al***

**Critical steps and hypothesis are partially verified (not conclusive) by X-ray tomography and 1-D Electron Cyclotron Emission (ECE)**

# Electron cyclotron emission



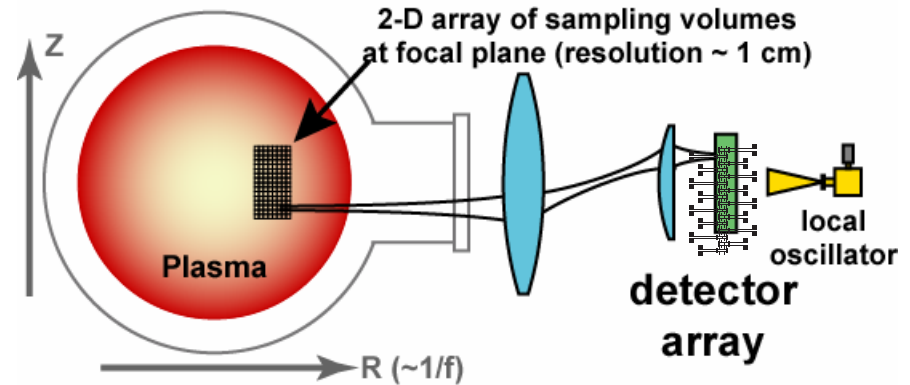
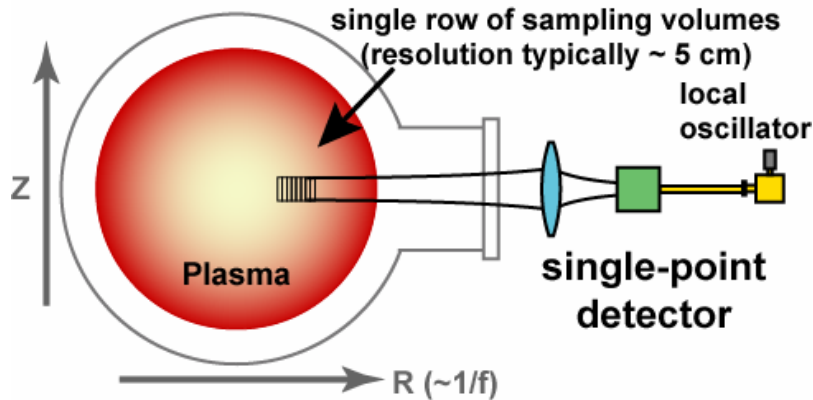
□ Electromagnetic (EM) waves are emitted at the electron cyclotron resonance (ECR) layer at a series of discrete harmonic frequencies:

□  $\omega_n = n\omega_{ce}$ ,  $\omega_{ce}(R) \propto B \propto 1/R$

□ If the plasma is Maxwellian and optically thick, the emission can be described as blackbody radiation in the Rayleigh-Jeans limit

□ Intensity:  $I(\omega) = I_B(\omega) \approx \frac{T_e \omega^2}{8\pi^3 c^2}$

# Microwave camera with zoom lens



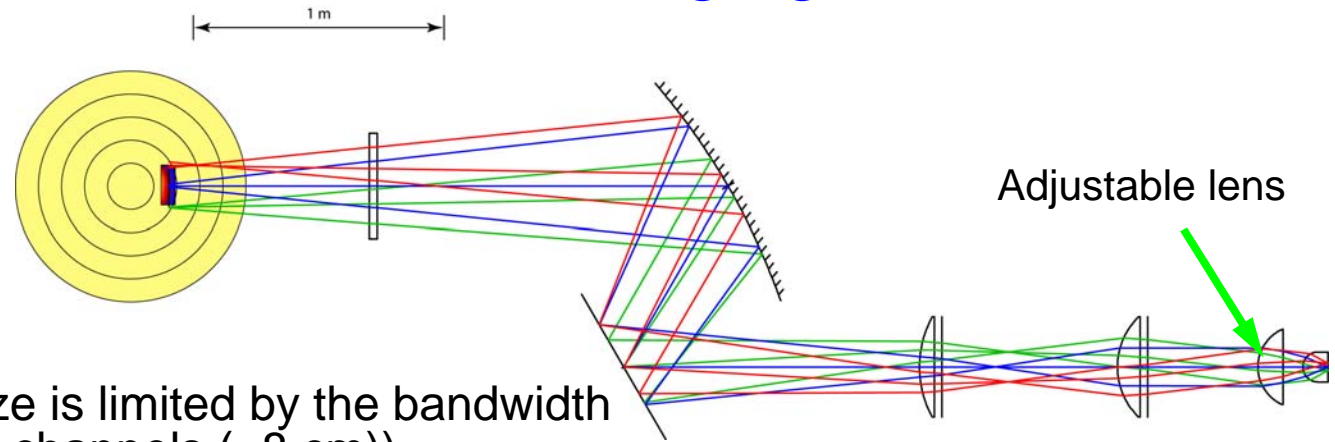
## Conventional 1-D ECE system

## 2-D ECE imaging system

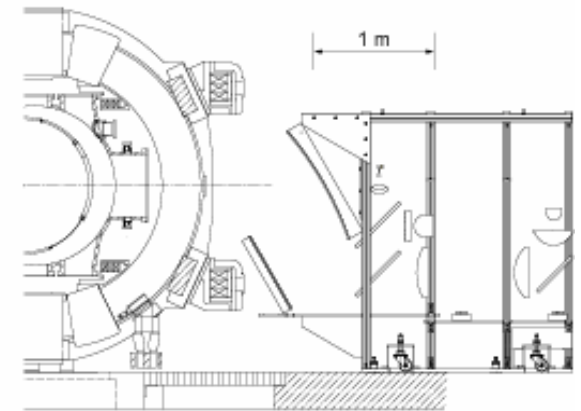
- ❑ ECE measurement is an established tool for electron temperature measurement in high temperature plasmas
- ❑ Sensitive 1-D array detector, imaging optics, and wide-band mm wave antenna, and IF electronics are required for 2-D imaging system
- ❑  $T_e$  fluctuation measurement
  - ❑ Real time fluctuations can be studied up to ~1% level
  - ❑ Fluctuation studies down to 0.1 % level have been performed using long time integration

# Characteristics of 2-D ECEI imaging on TEXTOR

128 channels  
(16 x 8)  
Spatial resolution  
(2 cm x 1 cm)  
Time resolution =  
5  $\mu$ sec.



- ❑ Radial image size is limited by the bandwidth of the system (8 channels (~8 cm))
  - ❑ LO frequency and/or B field change can extend the radial coverage
- ❑ Poloidal image size is limited by front end optics designed for MIR (16 channels (~16 cm))
- ❑ Relatively calibrated for fluctuation study  $\Delta T_e(r,t)/\langle T_e(r,t) \rangle$ ;  $\langle \rangle$  is time average temperature and constant for this study
  - ❑ Time resolution; ~ 5  $\mu$ s
  - ❑ Real time signal at ~1% level of  $T_e$  fluctuation (~10eV)
  - ❑ Sub ~1% level of fluctuation was studied with integration time



ECEI/MIR system on TEXTOR

# Relevant TEXTOR plasma parameters

## Global parameters:

$$B_T = 2.3T \quad I_p = 400kA \quad \beta_T \approx 1.0\%$$

$$B_p(a) \approx 1.6kG \quad P_{nbi} \approx 3MW \quad \beta_p \approx 0.4$$

## Plasma parameters:

$$V_A(B_T) \approx 3.8 \times 10^8 \text{ cm/s}$$

$$V_A(B_p) \approx 1.7 \times 10^7 \text{ cm/s}$$

$$V_{the} \approx 2.0 \times 10^9 \text{ cm/s}$$

$$C_s \approx 3.5 \times 10^7 \text{ cm/s}$$

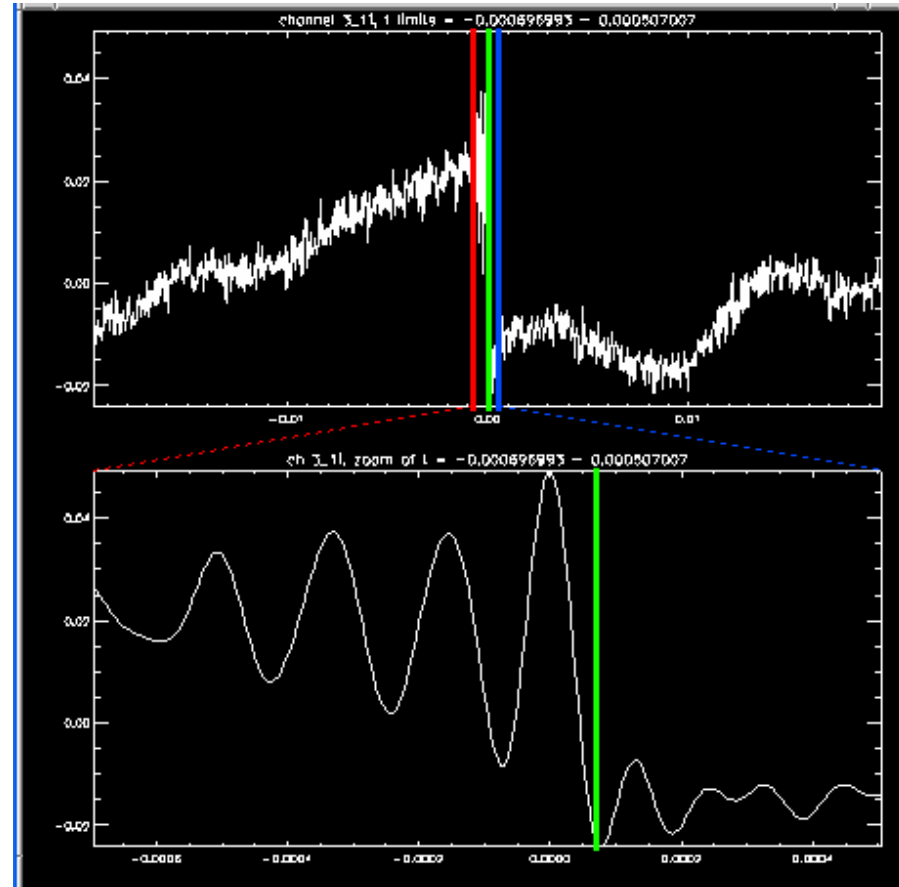
$$V_{rot} \approx 6.5 \times 10^6 \text{ cm/s}$$

$$\eta \approx 1.3 \times 10^{-6} \text{ ohm} \cdot \text{cm}$$

$$\frac{\Delta T_e}{\langle T_e \rangle}$$

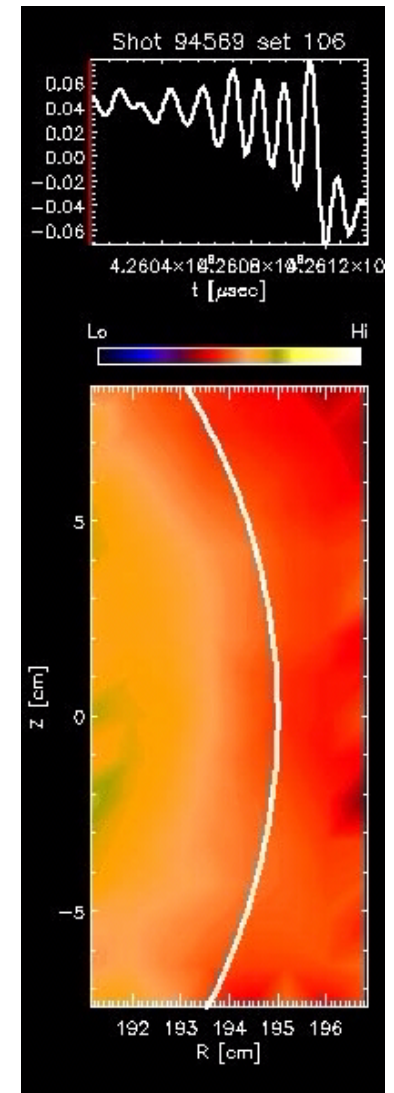
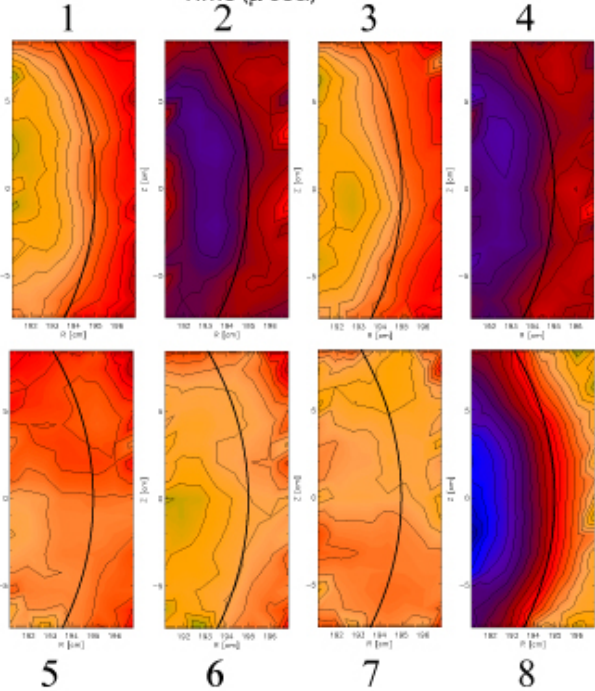
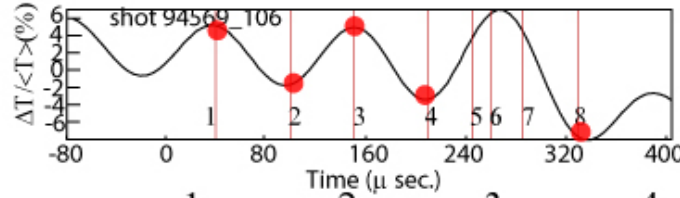
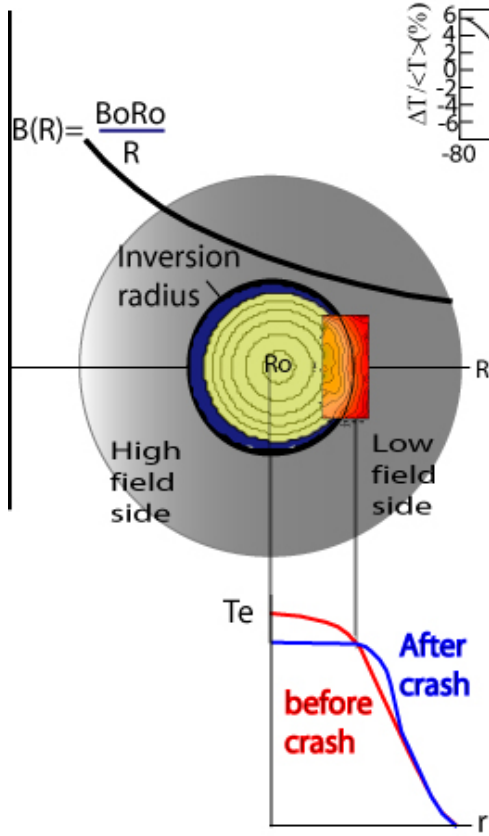
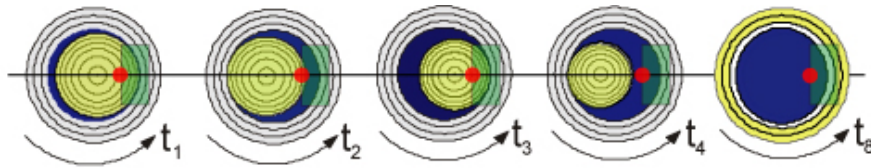
## full reconnection time:

$$\tau_k \approx \frac{1}{2} \sqrt{\tau_A^* \cdot \tau_\eta} \approx 650 \mu\text{sec.}$$



Time( $\mu\text{sec}$ )

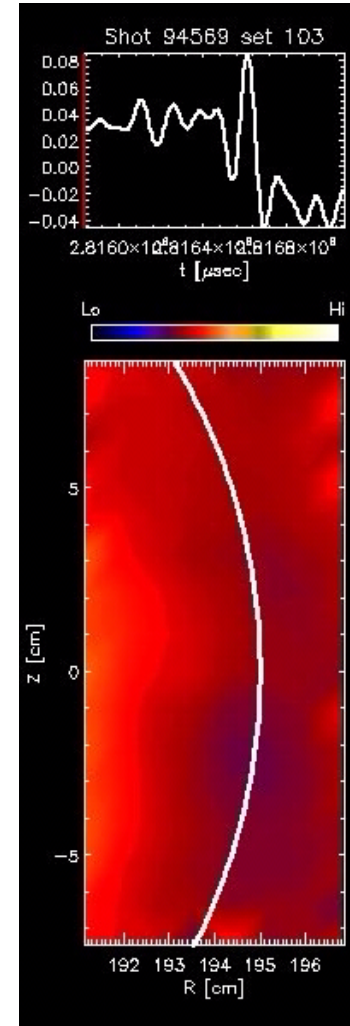
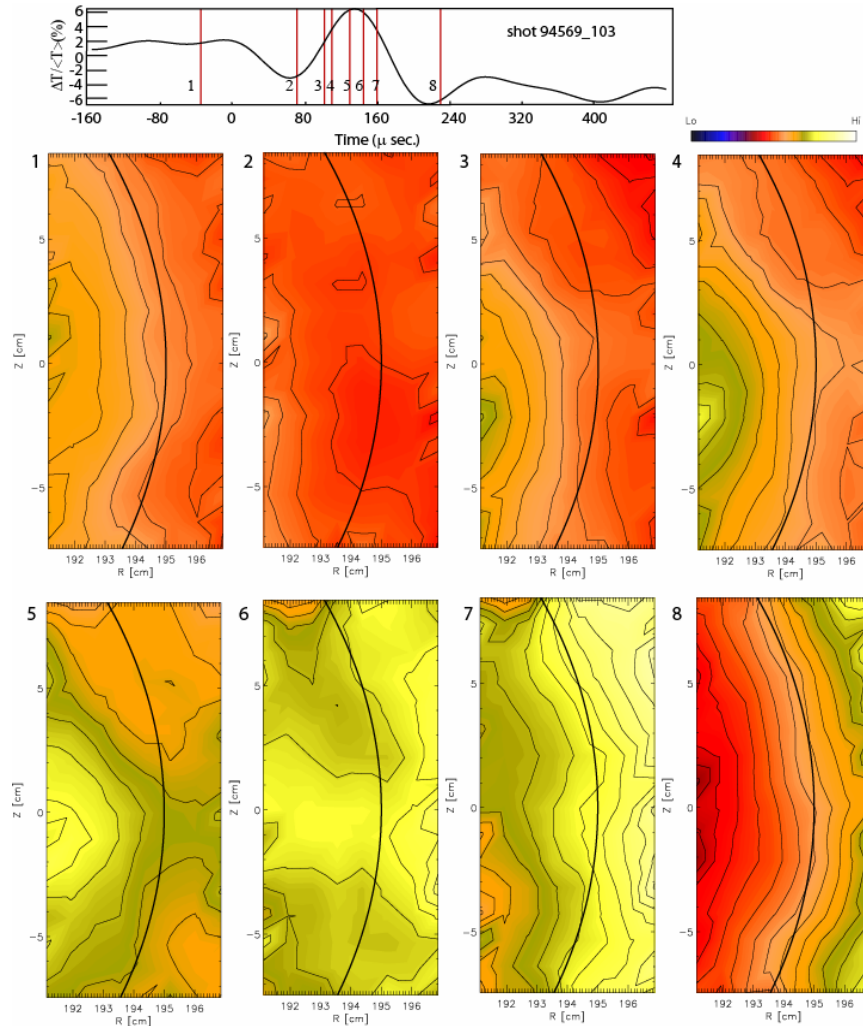
# Reconnection process via visualization





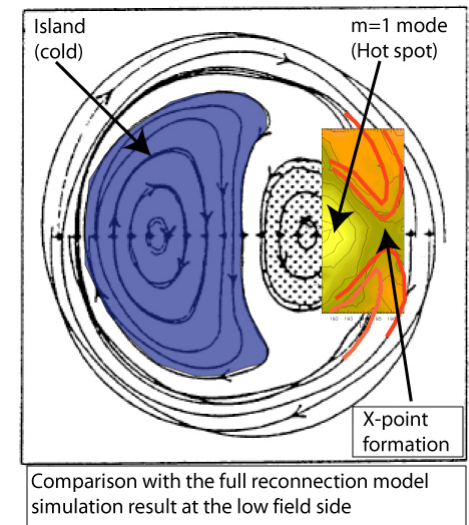
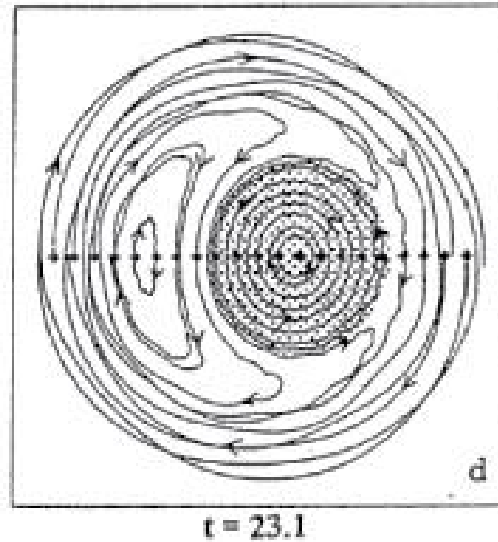
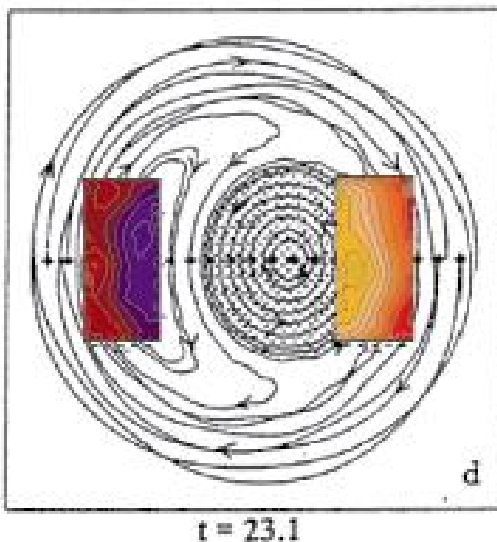
# Reconnection (“x-point”) at low field side

- Sharp  $T_e$  point (#4) is similar to the “Pressure Finger” of the Ballooning mode
- Reconnection starts with “X-point” (#5) and the poloidal opening grows to ~15 cm (#6)
- Reconnection at the low field side is consistent with the pressure driven Ballooning model
- Reconnection time scale is  $< 100\mu\text{s}$



# Comparison with the full reconnection model

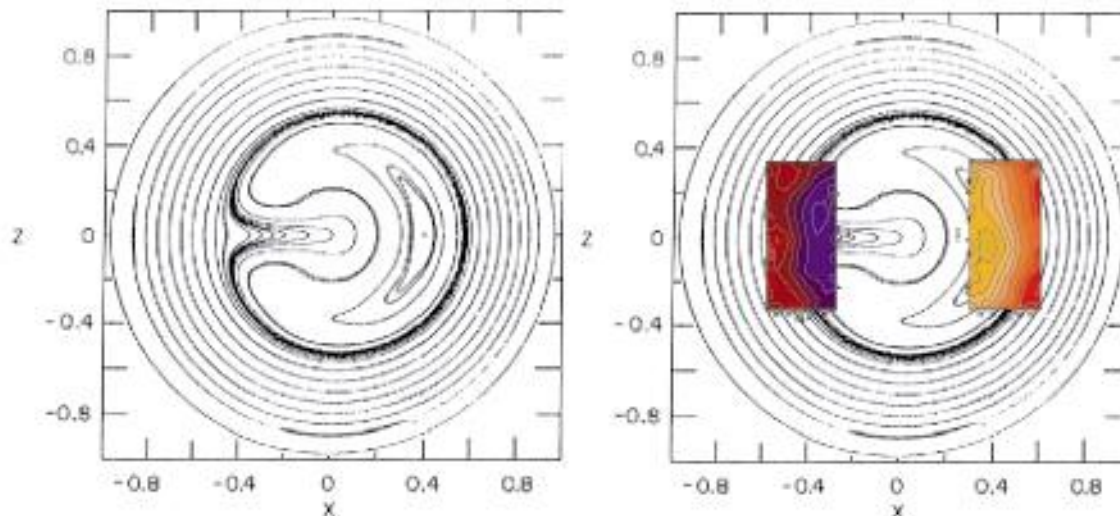
- ❑ Remarkable resemblance between 2-D images of the hot spot/Island and images from the mature stage of the simulation result of the full reconnection model (tearing type) (Sykes et al. single fluid MHD model)
  - ❑ Magnetic topology change (reconnection) occurred as the island is formed (slow reconnection)
  - ❑ No clear heat flow during precursor phase until a sharp temperature point is developed
  - ❑ Reconnection following the “sharp temperature point” forms “X-point”





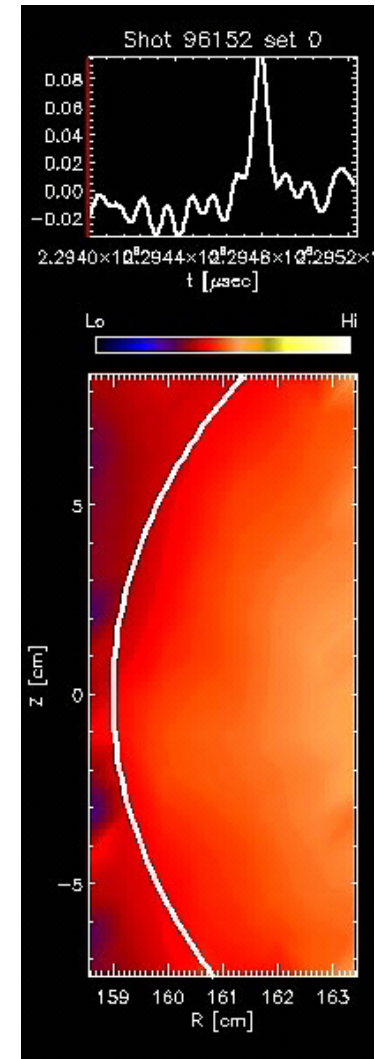
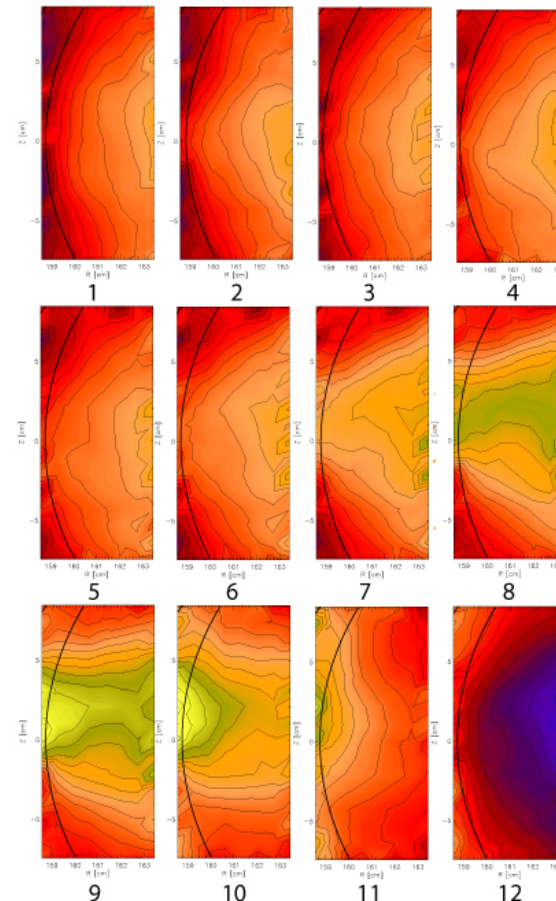
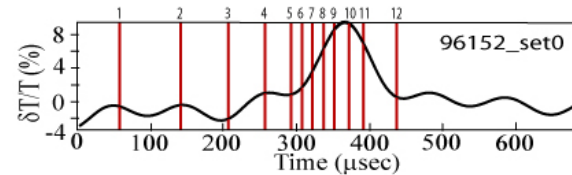
# Comparison with the quasi-interchange model

- No clear resemblance between 2-D images of hot spot/island and projected images from the quasi-interchange model
  - The observed images of the hot spot are close to circle not part of the crescent
  - The observed images of the island are vertically elongated shape, not oval shape
- This model does not require any type of magnetic field reconnection
  - Reconnection does occur following the pressure driven mode in the experiment.

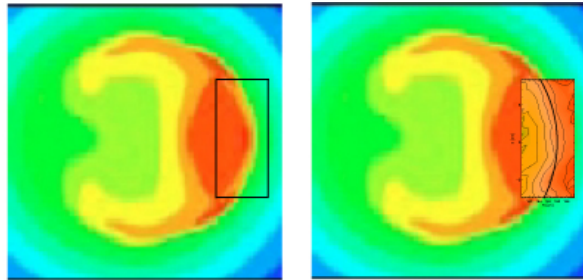


# Observation of the crash at high field side (kink)

- Reconnection is localized in poloidal plane similar to the low field case
- A few attempts (pointed  $T_e$  finger near the mid-plane) are made before the final puncture (#6 & #7)
- Reconnection starts with a small hole and it grows up to  $\sim 10$  cm (#10)
- Heat flow is highly collective similar to the low field case
- Nested field line pushes the heat out and island sets in (#11 and #12)

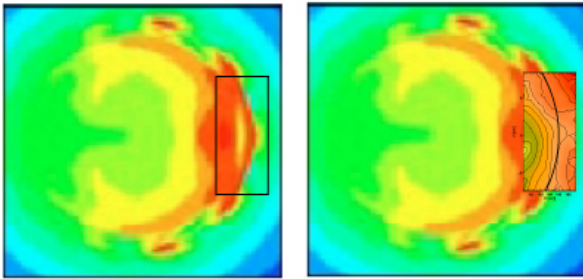


# Comparison with the ballooning mode model



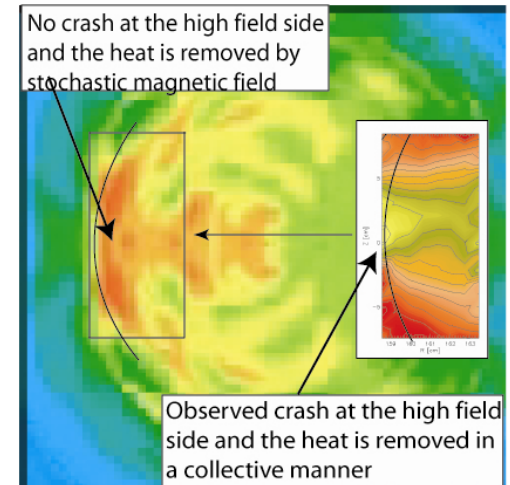
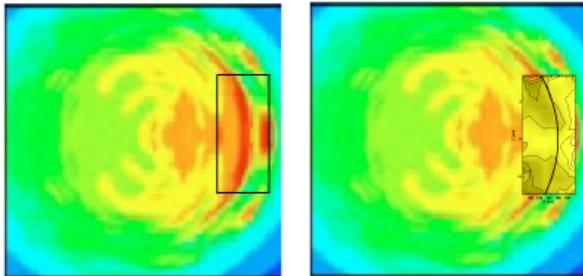
## □ Low field side

- Similarity: “Pressure finger” of the simulation at low field side (middle figure) is similar to those from 2-D images (“a sharp temperature point”)
- Difference: Heat flow is highly collective in experiment while stochastic process of the heat diffusion is clear in simulation.



## □ *High field side*

- *Reconnection at high field side is forbidden in Ballooning mode model*

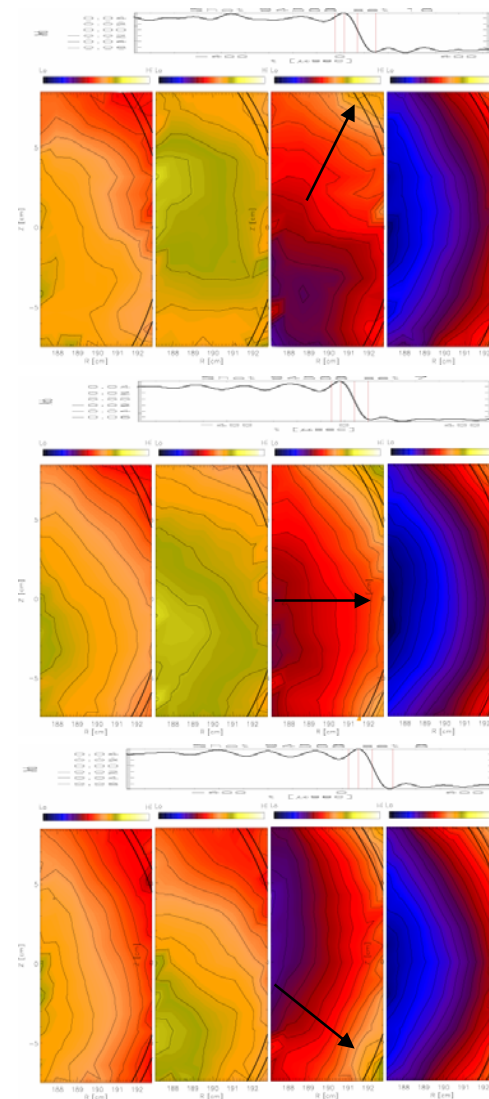
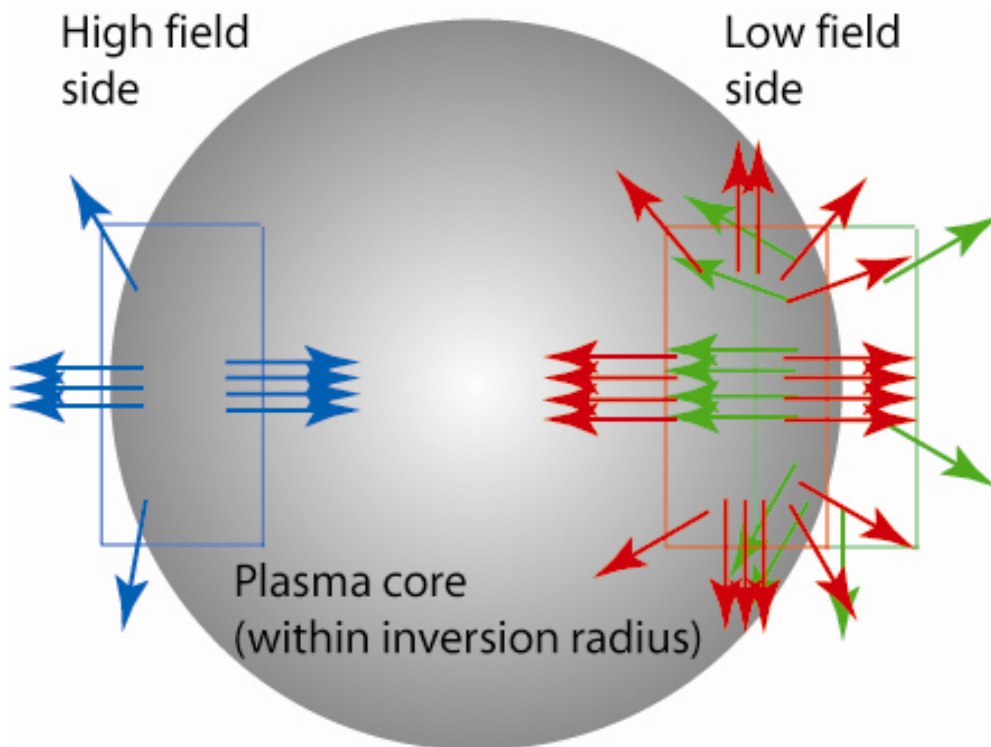


Comparison with the Ballooning model simulation result at the high field side

Simulation results from Nishimura et.al.  
Plasma condition ( $\beta_p \sim 0.4$  and  $\beta_t \sim 2\%$ )  
is similar to the experimental results

# Statistics of the crash pattern

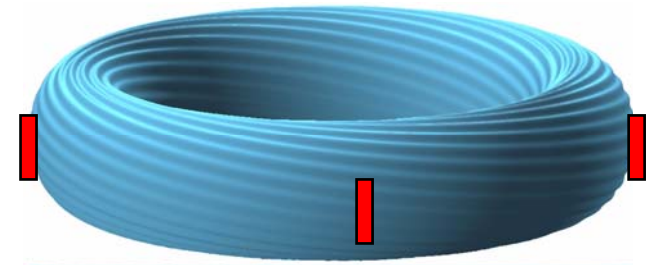
- ❑ Crash direction has been observed everywhere in high and low field sides
  - ❑ Effective poloidal view can be larger than the actual one (almost twice)



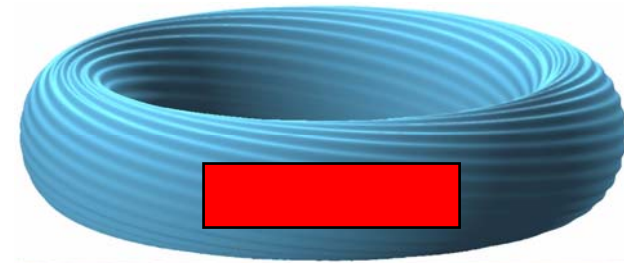


# Helical symmetry of the toroidal reconnection zone

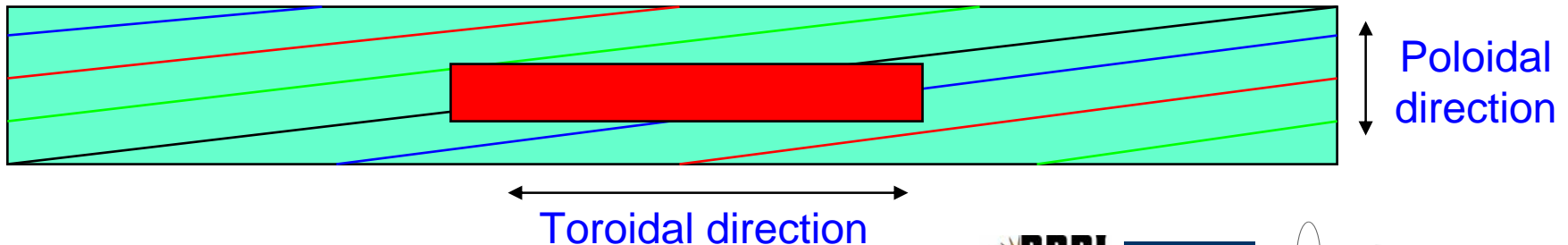
- Proof of helical symmetry of the toroidal reconnection zone
  - Requires multiple viewing along toroidal direction
- Rotating plasma provides an extended toroidal view
  - Window size is a function of the rotation speed
- Entire view can be projected on 2-D space spanned by poloidal and toroidal views



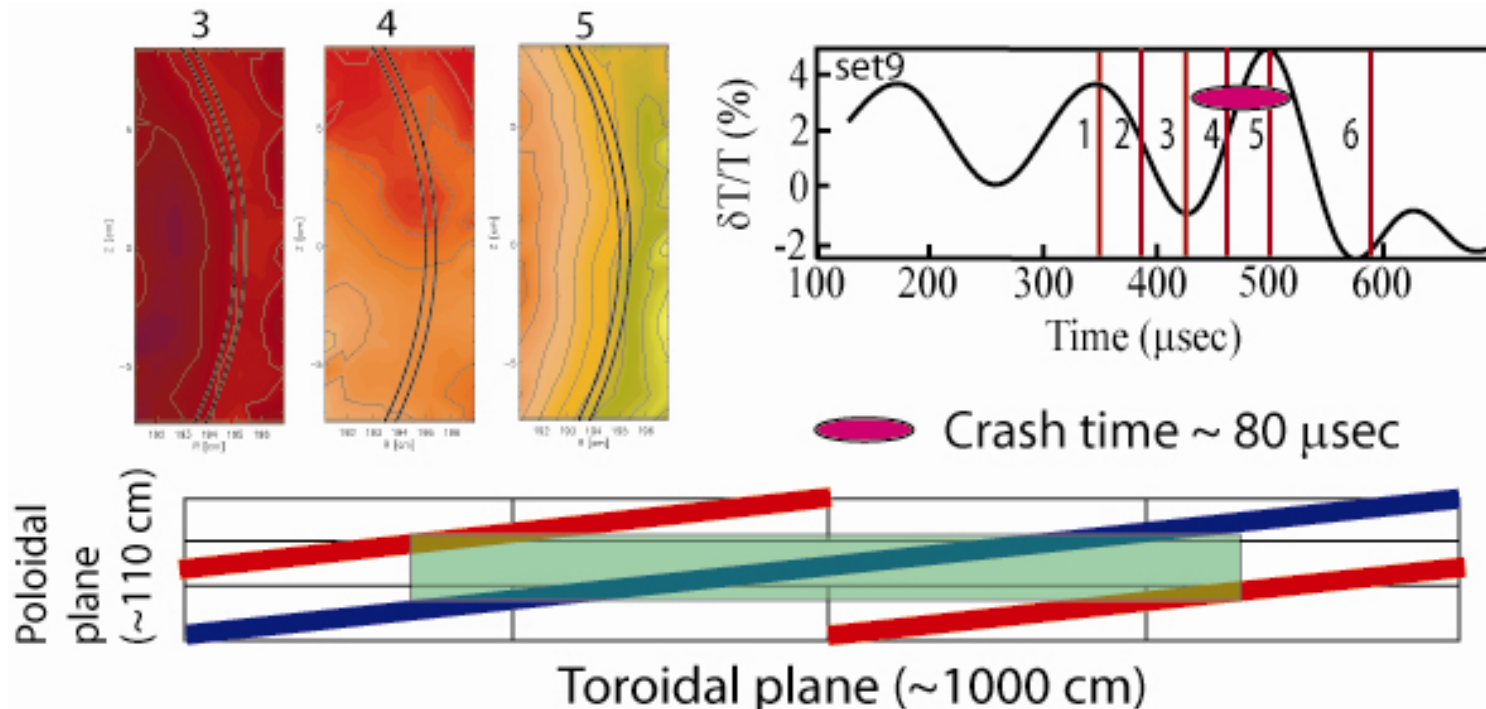
Stationary plasma



Rotating plasma

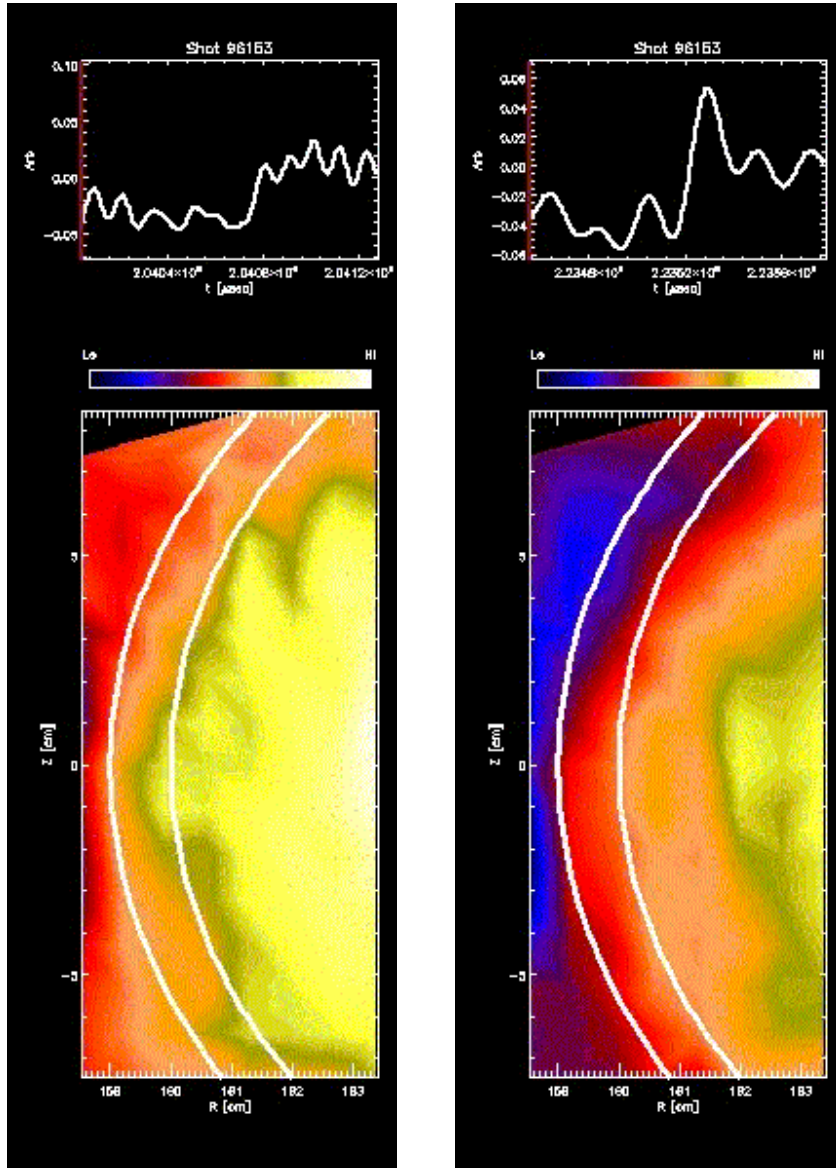


# Toroidal extent of the reconnection zone



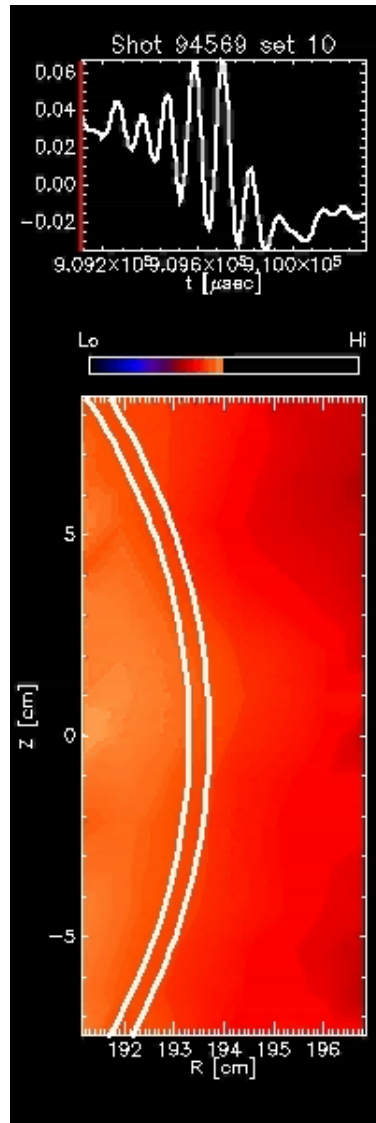
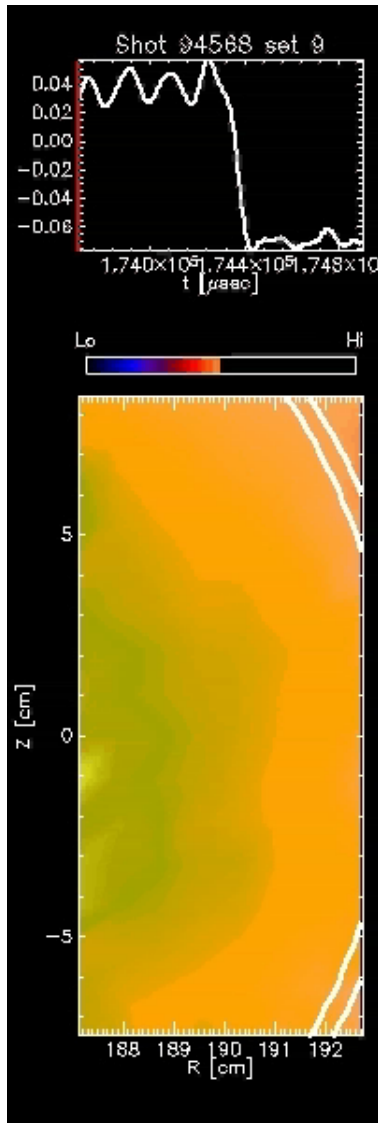
- ❑  $V_r \sim 7-8 \times 10^6 \text{ cm/sec}$  gives the toroidal window of  $\sim 650 \text{ cm}$  for the crash time ( $\sim 80 - 90 \mu\text{sec}$ )
- ❑ In a helically symmetric reconnection zone, chance of no reconnection zone in the viewing window is slim

# High field side crash (abnormal cases)



- Example of off-mid plane crash observed (right side) at high field side: 1-D measurement at the mid-plane will be difficult to interpret
- Hot spot runs away from high field side (indication of the crash other than at the high field side – left side): In a slowly rotating plasma, one may need two imaging systems to prove the helical symmetry

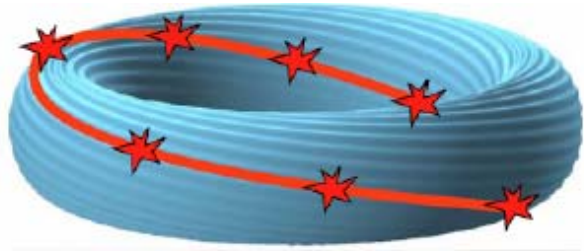
# Low field side crash (fast rotating plasmas)



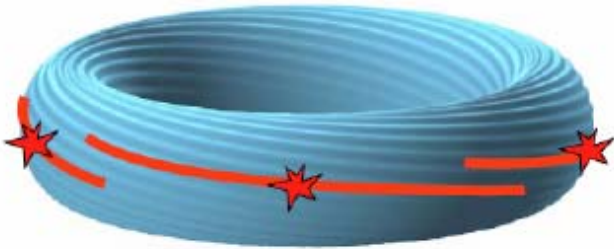
- Off-mid plane crash is also observed (right side) at the low field side (moving to the top)
- Crash pattern runs away from low field side (indication of the crash other than at the low field side – left side): **no trace of reconnection zone during whole crash time scale**
  - 1/4 of  $\sim 40$  frames has similar crash pattern
  - Reconnection event has to be not only localized but also random phenomenon



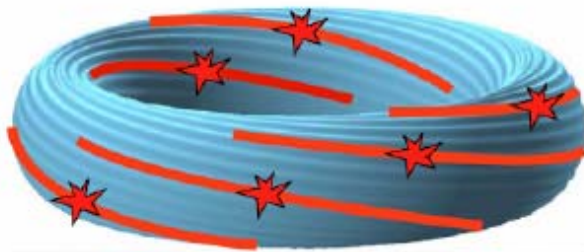
# Random 3-D localized reconnection



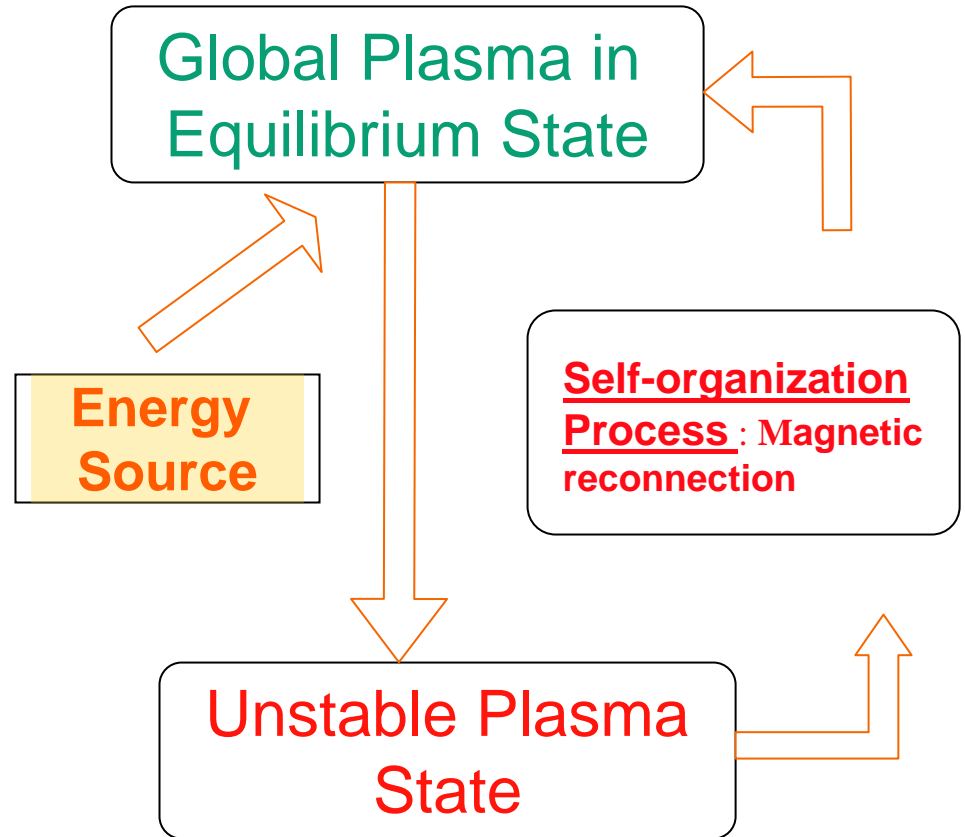
Full reconnection (Helically symmetric crash)



3-D Local reconnection (localized crash at low field side)



Random 3-D Local reconnection (localized crash everywhere)

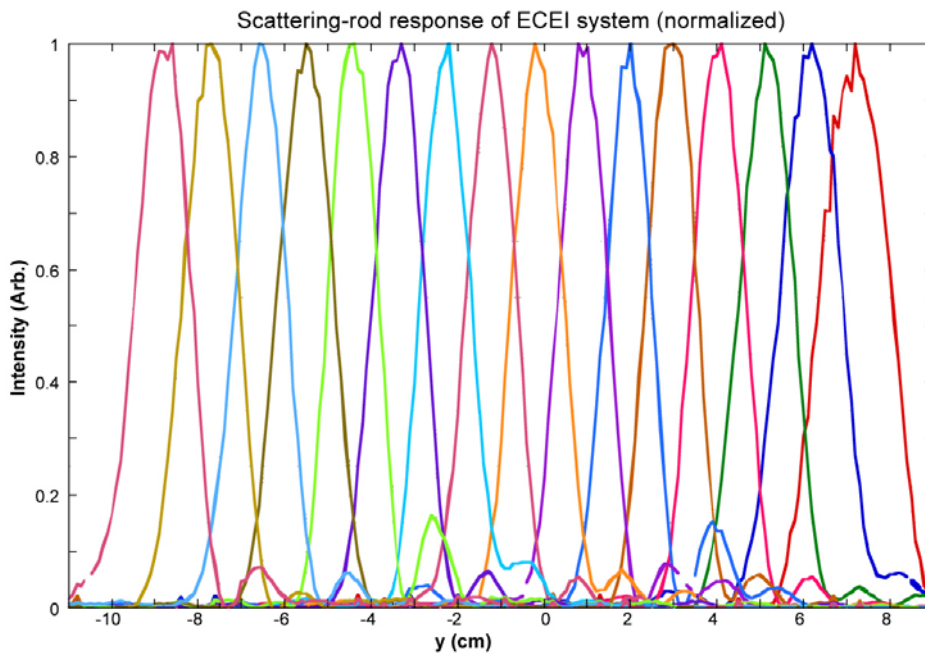
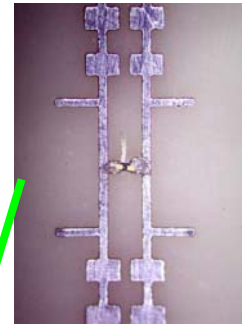


## Summary

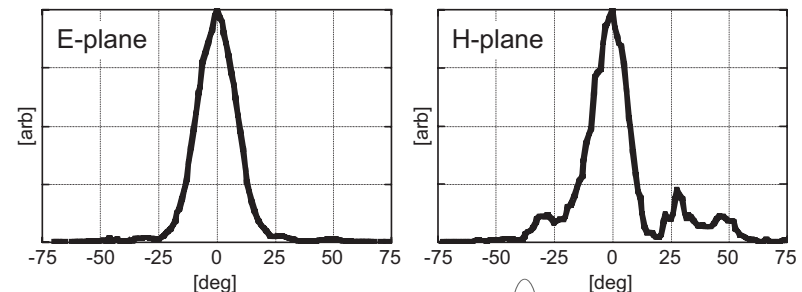
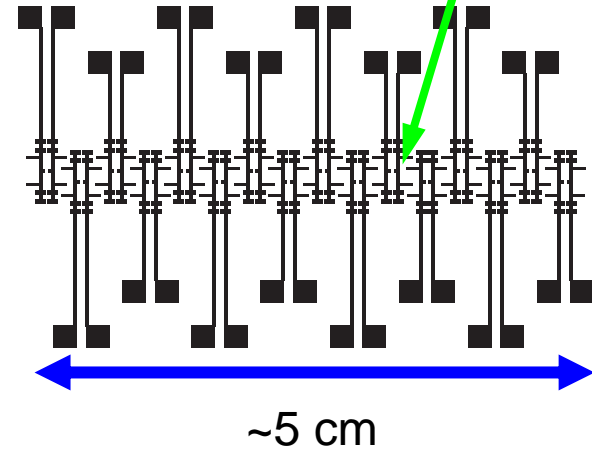
- ❑ No theoretical models are consistent with the measured 2-D images
  - ❑ Full reconnection model is largely consistent except
    - No reconnection before the pressure point develops
    - Assumption of the helical symmetry is not valid
  - ❑ Quasi-interchange model – Inconsistent with the measurement (magnetic instability is not likely a dominant mechanism)
  - ❑ Ballooning mode model is partly consistent except
    - 3-D random local reconnection process
    - Global stochasticity of the magnetic field line may not be dominant mechanism for the heat transport

# Advances in detector array technology

- Improved antenna patterns & power sensitivity of **dual dipole array** compared to those of the previously employed slot bow-tie array

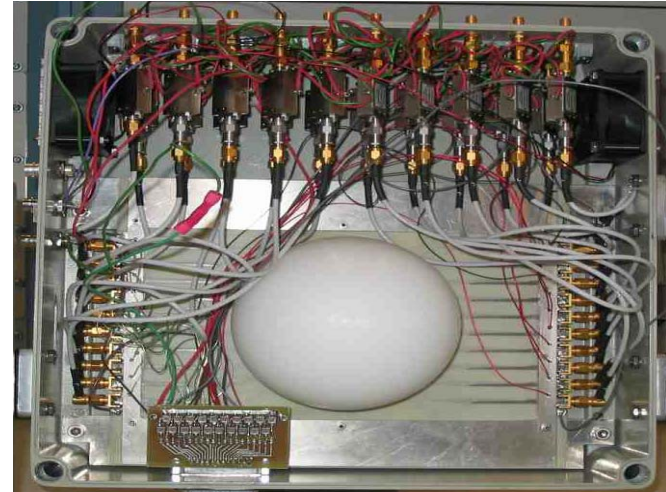


**ECEI system antenna response**

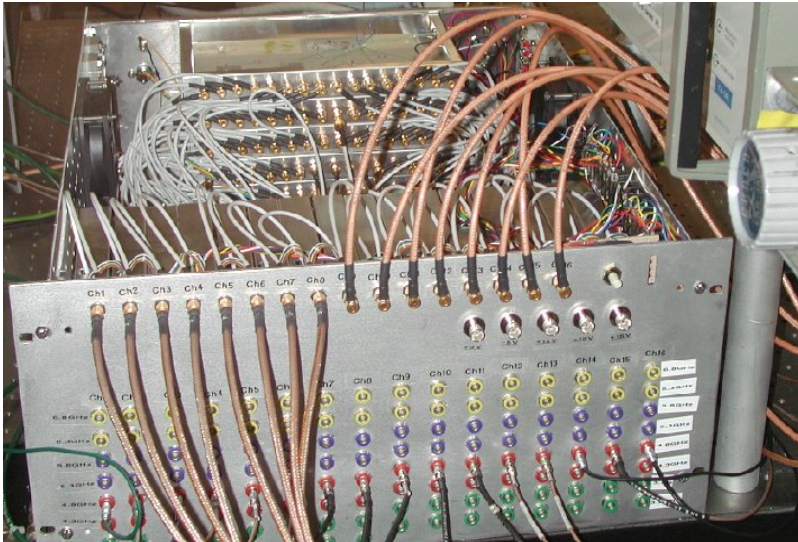


# Array box and electronics for ECEI system

- ❑ Completed detection array with the substrate lens and low-noise microwave pre-amplifiers.

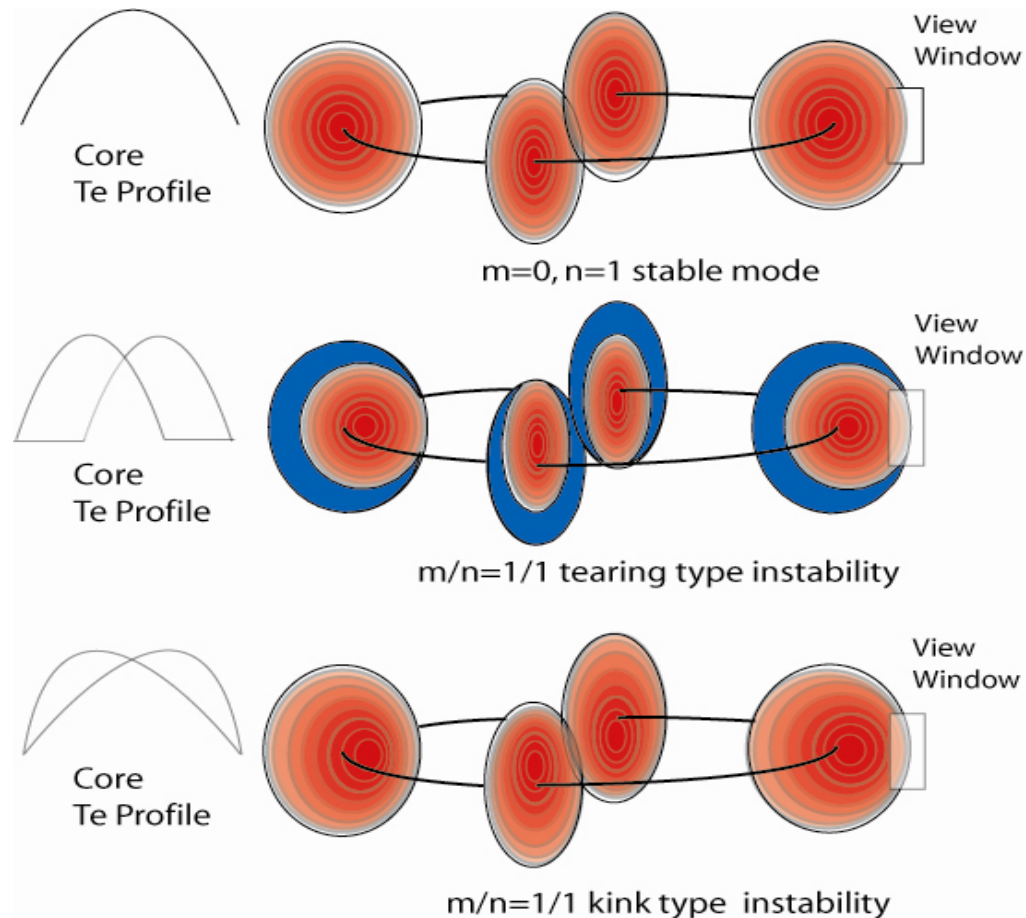


- ❑ Completed ECEI electronics box, with 16 SMA array inputs (3-7 GHz) and 128 LEMO outputs (8 outputs per input)



# Sawtooth instability

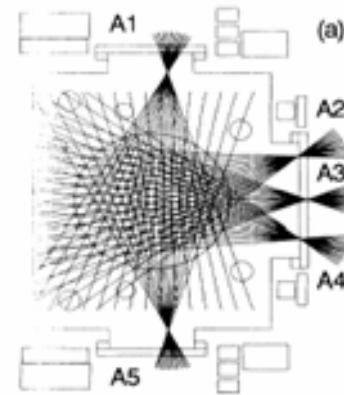
- Stable  $m/n=0/1$  mode in the initial stage
- $m/n=1/1$  mode develops as the instability grows (kink or tearing instability) and reconnection occurs
  - Tearing mode instability (slow evolution of the island/hot spot)
  - Kink mode instability (sudden crash)
- Reconnection time scale is any different in these two types ?





# Study of sawtooth oscillations by X-ray tomography

- ❑ X-ray tomography – Needs careful interpretation
  - ❑ X-ray tomography supports all theoretical models
    - *Quasi-interchange model; R. Granetz ('88)*
    - *Full reconnection and interchange models dependent upon polynomials: C. Janicki ('89)*
    - *Asymmetries in high & low field side supports 3-D local reconnection- : S. Yamaguchi ('04)*
- ❑ Reconstruction of 2-D and 3-D image from multiple arrays
  - *Inversion process is complex and unique solution may not be feasible in practice*
  - *Parametric dependence of the X-ray signal adds more complexity ( $T_e$ ,  $n_e$  and  $Z_{eff}$ )*



C. Janicki et al

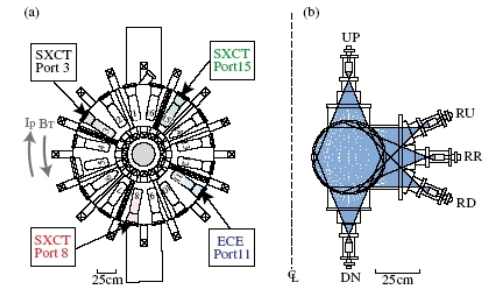


FIG. 1 (color online). (a) Top view of the WT-3 tokamak. (b) Cross-sectional view of the SXCT system.

S. Yamaguchi et al

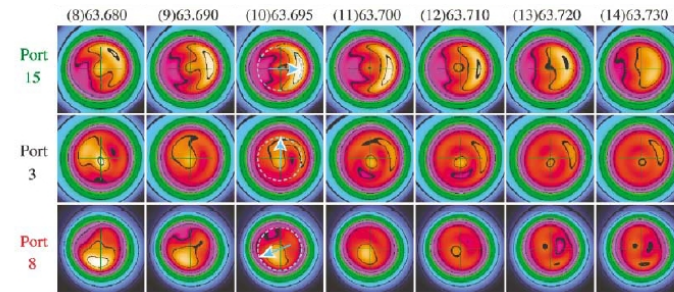


FIG. 2 (color). Time evolutions of the SX images at three ports. In each SX image, the left side is the high field side. The dashed circles denote the inversion circle with  $r_{inv} = 63$  mm.

*As the reconnection at the low field side (port #15) is progressing, no clear actions in other ports.*